Electronic Research Archive

https://www.aimspress.com/journal/era

ERA, 32(7): 4433–4453.
DOI: 10.3934/era.2024200
Received: 17 April 2024
Revised: 29 June 2024
Accepted: 08 July 2024
Published: 15 July 2024

*Research article*

# Hamiltonian conserved Crank-Nicolson schemes for a semi-linear wave equation based on the exponential scalar auxiliary variables approach

**Huanhuan Li, Lei Kang, Meng Li, Xianbing Luo* and Shuwen Xiang**

School of Mathematics and Statistics, Guizhou University, Guiyang 550025, China

* **Correspondence:** Email: xbluo1@gzu.edu.cn.

**Abstract:** The keys to constructing numerical schemes for nonlinear partial differential equations are accuracy, handling of the nonlinear terms, and physical properties (energy dissipation or conservation). In this paper, we employ the exponential scalar auxiliary variable (E-SAV) method to solve a semi-linear wave equation. By defining two different variables and combining the Crank−Nicolson scheme, two semi-discrete schemes are proposed, both of which are second-order and maintain Hamiltonian conservation. Two numerical experiments are presented to verify the reliability of the theory.

**Keywords:** semi-linear wave equation; exponential scalar auxiliary variable; error analysis; Crank−Nicolson scheme

## 1. Introduction

Nonlinear partial differential equations (PDEs) are often used to describe some significant problems in natural science and engineering technology. The analysis of nonlinear waves has garnered increasing attention in the fields of shallow water, plasma, nonlinear optics, Bose−Einstein condensates, and fluids. The nonlinear PDEs in these fields can be solved using lump solutions. The lump solution and interaction hybrid solutions were first discovered by Zakharov in [1] and Craik in [2], respectively. These special solutions are of great significance for the study of nonlinear integrable equations [3–5]. To obtain these analytical solutions, the scholars have proposed a variety of methods, including Ansatz technique [6], Hirota's bilinear method (HBM) [7], and the inverse scattering transform (IST) [8]. The HBM proposed by Hirota, has been widely used as an effective approach to study the nonlinear dynamics wave equation, resulting in numerous richer solutions, such as solitons solutions, novel breather waves, lump solutions, two-wave solutions, and rogue wave solutions ( [9–14]). These solutions are visualized in three-dimensional graphics via numerical simulations, making it easier to understand the propagation of nonlinear waves.

The study of the stability of integrable equations, such as the KPI equation, the Ishimori equation, the nonlinear Schrödinger (NLS) equation and the KdV equation have further enriched the theory of nonlinear wave equations. Spectral methods can effectively solve the problem of linear stability. In [15], Degasperis et al. proposed the construction of the eigenmodes of the linearized equation using the associated Lax pair and provided the computation of both analytical and numerical solutions with the example of two coupled NLS equations. In [16], Ablowitz provided a comprehensive review of research methods for integrability and nonlinear waves, including Bäcklund transformations, Darboux transformations, direct integral equations or Riemann−Hilbert or Dbar methods, and HBM. By combining the KdV and NLS equations, the author further elaborated on the ideas and background of the IST method.

The computation of nonlinear PDEs has become a very active research topic. With advancements in traditional methods like finite element ( [17, 18]), finite difference ( [19–24]), finite volume ( [25–27]), and spectral methods ( [28–30]), numerous outstanding research results have been achieved in the numerical approximations of nonlinear PDEs. In [31], the authors developed a time-two-grid difference scheme for nonlinear Burgers equations. In [32], a method combining the barycentre Lagrange interpolation collocation technique with a second-order operator splitting approach was proposed for the purpose of solving the NLS equation. Based on novel shifted Delannoy functions, Ansari et al. [33] employed a matrix collocation technique to numerically approximate the singularly perturbed parabolic convection−diffusion−reaction problems.

In recent years, for the treatment of nonlinear terms, there have been a lot of unconditionally energy dissipative numerical schemes for Allen−Cahn and Cahn−Hilliard gradient flows models, such as:
(i) CSS (convex splitting) scheme [34–36];
(ii) IMEX (stabilized semi-implicit) scheme [37, 38];
(iii) ETD (exponential time differencing) scheme [39, 40];
(iv) IEQ (invariant energy quadratization) scheme [41];
(v) SAV (scalar auxiliary variable) scheme [42, 43];
(vi) E-SAV (exponential scalar auxiliary variable) scheme [44].

The idea of (i) is to decompose the energy function into convex and concave parts, handling the convex part implicitly and the concave part explicitly. The advantage is that it can achieve second-order unconditional stability. However, the drawback is that it still requires solving nonlinear equations. The method of (ii) yields extra error, which makes it difficult to construct a higher-order scheme. The (iv) and (v) approaches make it easier to handle nonlinear terms by defining auxiliary variables that transform the nonlinear potential function into a simple quadratic form. Nevertheless, an inner product must be calculated before obtaining the next time value. Compared with (iv) and (v), the variable defined in (vi) does not require any assumptions. And the E-SAV method can easily construct an explicit scheme that can preserve energy stability. But this physical property can not be satisfied with the explicit SAV scheme.

In addition, Huang et al. [45] studied a new SAV method to approximate the gradient flows, which is an improvement of the SAV method. By defining an auxiliary variable in the new SAV method as a shifted total energy function, instead of focusing on the nonlinear parts of the classic SAV method, we replace the dynamic equation for that variable with the energy balance equation of the gradient flow. This facilitates the construction of high-order and energy-stable discrete schemes. In [46], Liu et al. further developed an exponential semi-implicit scalar auxiliary variable (ESI-SAV) method for the phase field equation. The ESI-SAV method can preserve the advantages of both the new SAV and

E-SAV methods and be applied more effectively to other dissipative systems.

On the basis of the above methods, researchers began to apply the above nonlinear processing techniques to approximate semi-linear wave equations. Jiang et al. [47] proposed an IEQ approach and established an energy-preserving linear implicit scheme for the sine-Gordon equation. In [48], based on the SAV method with a combination of the Gauss technique and the extrapolation method, Li et al. provided a high-order energy-conserving and linearly implicit scheme. Wang et al. [49] developed a second-order SAV Fourier spectral method to solve a nonlinear fractional generalized wave equation.

The primary objective of this paper is to develop second-order and Hamiltonian conserved semi-discrete schemes for semi-linear wave equations. Following the superiorities of the E-SAV and ESI-SAV methods, two different numerical schemes are given by utilizing the Crank−Nicolson scheme for temporal approximation. Furthermore, the convergence order and the evolution curve of the Hamiltonian function are validated through numerical experiments.

The paper is organized as follows: In Section 2, by introducing scalar auxiliary variables, we obtain two equivalent forms for the semi-linear wave equation in the continuous case. In Sections 3 and 4, by using the Crank−Nicolson scheme, we propose two semi-discrete schemes corresponding to the equivalent forms and provide proof of the convergence order. Two numerical examples are implemented to test the effectiveness of the theoretical analysis in Section 5.

## 2. Preliminary results

We consider the following semi-linear wave equation:

$$\begin{cases} y_{tt} - \Delta y - f(y) = 0, & \boldsymbol{x} \in \Omega, t \in (0,T), \\ y(\boldsymbol{x},t) = 0, & \boldsymbol{x} \in \partial\Omega, t \in (0,T), \\ y(\boldsymbol{x},0) = y_0(\boldsymbol{x}), y_t(\boldsymbol{x},0) = g(\boldsymbol{x}), & \boldsymbol{x} \in \Omega, \end{cases} \tag{2.1}$$

where $\Omega \subset \mathbb{R}^d (d = 2, 3)$ is a bounded convex domain, $T > 0$ is a fixed number, $f(y) = -F'(y)$ is a nonlinear term, and $F(y)$ satisfies $F(y) \in C^3(R)$. The Hamiltonian function is defined as

$$H(y) = \frac{1}{2}\|y_t\|^2 + \frac{1}{2}\|\nabla y\|^2 + \int_\Omega F(y) d\boldsymbol{x}. \tag{2.2}$$

**Proposition 2.1.** *The system* (2.1) *holds the following Hamiltonian conservation law:*

$$\frac{dH(y)}{dt} = 0. \tag{2.3}$$

*Proof.* Multiplying the first equation of the system (2.1) by $y_t$ yields

$$y_{tt}y_t - \Delta y y_t - f(y)y_t = 0. \tag{2.4}$$

By using the continuous Leibniz rule, we obtain

$$y_{tt}y_t = \frac{1}{2}\left((y_t)^2\right)_t, \quad -f(y)y_t = (F(y))_t, \tag{2.5}$$

and

$$\Delta y y_t = (y_{x_1x_1} + y_{x_2x_2})y_t$$

$$
\begin{aligned}
&=(y_{x_1}y_t)_{x_1} + (y_{x_2}y_t)_{x_2} - y_{x_1}(y_t)_{x_1} - y_{x_2}(y_t)_{x_2} \\
&=(y_{x_1}y_t)_{x_1} + (y_{x_2}y_t)_{x_2} - \frac{1}{2}(y_{x_1}^2 + y_{x_2}^2)_t.
\end{aligned} \tag{2.6}
$$

Inserting (2.5) and (2.6) into (2.4), we obtain

$$
\left[\frac{1}{2}\left((y_t)^2\right)_t + \frac{1}{2}\left(y_{x_1}^2 + y_{x_2}^2\right)_t + (F(y))_t\right] - \left[(y_{x_1}y_t)_{x_1} + (y_{x_2}y_t)_{x_2}\right] = 0. \tag{2.7}
$$

Integrating (2.7) over the spatial domain Ω and combining the boundary conditions leads to

$$
\int_\Omega \left[\frac{1}{2}\left((y_t)^2\right)_t + \frac{1}{2}(y_{x_1}^2 + y_{x_2}^2)_t + (F(y))_t\right] d\boldsymbol{x} = 0, \tag{2.8}
$$

From (2.8) and (2.2), we can deduce that

$$
\frac{dH(y)}{dt} = \int_\Omega \left[\frac{1}{2}\left((y_t)^2\right)_t + \frac{1}{2}(y_{x_1}^2 + y_{x_2}^2)_t + (F(y))_t\right] d\boldsymbol{x} = 0. \tag{2.9}
$$

The proof is complete.

We introduce two scalar auxiliary variables as

$$
\omega = y_t, \ r(t) = \int_\Omega F(y) d\boldsymbol{x} = \mathcal{H}_2(y).
$$

Then the system (2.1) can be equivalently rewritten as

$$
\begin{aligned}
&\omega = y_t, && \boldsymbol{x} \in \Omega, t \in (0, T), && (2.10)\\
&\omega_t - \Delta y - q^{y,r} f(y) = 0, && \boldsymbol{x} \in \Omega, t \in (0, T), && (2.11)\\
&r_t = -q^{y,r}(f(y), \omega), && \boldsymbol{x} \in \Omega, t \in (0, T), && (2.12)\\
&y(\boldsymbol{x}, t) = 0, \ \ \omega(\boldsymbol{x}, t) = 0, && \boldsymbol{x} \in \partial\Omega, t \in (0, T), && (2.13)\\
&y(\boldsymbol{x}, 0) = y_0(\boldsymbol{x}), \ \ \omega(\boldsymbol{x}, 0) = g(\boldsymbol{x}), \ \ r(0) = \mathcal{H}_2(y_0(\boldsymbol{x})), && \boldsymbol{x} \in \Omega, && (2.14)
\end{aligned}
$$

where

$$
q^{y,r} = \frac{\exp\{r\}}{\exp\{\mathcal{H}_2(y)\}}.
$$

For the system (2.10)–(2.14), we have the following lemma:

**Lemma 2.1.** *( Hamiltonian conservation) The above system* (2.10)–(2.14) *satisfies*

$$
\frac{d\tilde{\mathcal{H}}(y)}{dt} = 0, \tag{2.15}
$$

*where the modified Hamiltonian function*

$$
\tilde{H}(t) = \frac{1}{2}\|\omega\|^2 + \frac{1}{2}\|\nabla y\|^2 + r. \tag{2.16}
$$

*Proof.* Taking the inner product of (2.11) by $\omega$, then combining (2.10) and (2.12), we obtain

$$(\omega_t, \omega) + (\nabla y, \nabla y_t) + r_t = 0.$$

Obviously, we can deduce

$$\frac{d}{dt}\left(\frac{1}{2}\|\omega\|^2 + \frac{1}{2}\|\nabla y\|^2 + r\right) = 0.$$

The proof is complete.

Next, introducing a new variable

$$\mathcal{R}(t) = H(y),$$

which satisfies the dissipation law

$$\frac{d\mathcal{R}}{dt} = \frac{dH(y)}{dt} = 0, \tag{2.17}$$

and defining $\xi = \frac{\exp(\mathcal{R})}{\exp(H(y))}$, we can know that $\xi \equiv 1$ in the continuous case. Replacing the factor $q^{y,r}$ in (2.11) by $Q(\xi)$, where $Q(\xi)$ is a polynomial function of $\xi$, the system (2.1) can be transformed into the following equivalent form:

$$\omega = y_t, \qquad \boldsymbol{x} \in \Omega, t \in (0, T), \tag{2.18}$$

$$\omega_t - \Delta y - Q(\xi) f(y) = 0, \qquad \boldsymbol{x} \in \Omega, t \in (0, T), \tag{2.19}$$

$$\xi = \frac{\exp(\mathcal{R})}{\exp(H(y))} \qquad \boldsymbol{x} \in \Omega, t \in (0, T), \tag{2.20}$$

$$Q(\xi) = \xi(2 - \xi) \qquad \boldsymbol{x} \in \Omega, t \in (0, T), \tag{2.21}$$

$$\frac{dR}{dt} = 0, \qquad \boldsymbol{x} \in \Omega, t \in (0, T), \tag{2.22}$$

$$y(\boldsymbol{x}, t) = 0, \ \ \omega(\boldsymbol{x}, t) = 0, \qquad \boldsymbol{x} \in \partial\Omega, t \in (0, T), \tag{2.23}$$

$$y(\boldsymbol{x}, 0) = y_0(x), \ \ \omega(\boldsymbol{x}, 0) = g(\boldsymbol{x}), \ \ \mathcal{R}(0) = H(y_0), \qquad \boldsymbol{x} \in \Omega. \tag{2.24}$$

Furthermore, (2.17) and (2.22) imply that the system (2.18)–(2.24) is Hamiltonian conserved.

## 3. CN-E-SAV scheme

Let $0 = t_0 < t_1 < ... < t_N = T$ be a uniform partition of the time interval $[0, T]$ with the time steps $\Delta t = T/N$ and $t^n = n\Delta t$. Then, utilizing the Crank−Nicolson scheme to discretize the system (2.10)–(2.14), a second-order Carnk−Nicolson E-SAV (**CN-E-SAV**) scheme can be formulated as follows:

$$\omega^{n+\frac{1}{2}} = \frac{1}{\Delta t}(y^{n+1} - y^n), \tag{3.1}$$

$$\frac{1}{\Delta t}(\omega^{n+1} - \omega^n) - \Delta y^{n+\frac{1}{2}} - \hat{q}^{n+\frac{1}{2}} f(\hat{y}^{n+\frac{1}{2}}) = 0, \tag{3.2}$$

$$\frac{1}{\Delta t}(r^{n+1} - r^n) = -(\hat{q}^{n+\frac{1}{2}} f(\hat{y}^{n+\frac{1}{2}}), \omega^{n+\frac{1}{2}}), \tag{3.3}$$

where

$$\omega^{n+\frac{1}{2}} = \frac{1}{2}(\omega^{n+1} + \omega^n),\ y^{n+\frac{1}{2}} = \frac{1}{2}(y^{n+1} + y^n),$$

and $\hat{q}^{n+\frac{1}{2}} > 0$ with $(\hat{y}^{n+\frac{1}{2}}, \hat{r}^{n+\frac{1}{2}})$ being generated by the first-order scheme with the time step size $\frac{\Delta t}{2}$, i.e.,

$$\hat{\omega}^{n+\frac{1}{2}} = \frac{1}{\Delta t/2}(\hat{y}^{n+\frac{1}{2}} - y^n), \tag{3.4}$$

$$\frac{1}{\Delta t/2}(\hat{\omega}^{n+\frac{1}{2}} - \omega^n) - \Delta\hat{y}^{n+\frac{1}{2}} - q^n f(y^n) = 0, \tag{3.5}$$

$$\frac{1}{\Delta t/2}(\hat{r}^{n+\frac{1}{2}} - r^n) = -q^n(f(y^n), \hat{\omega}^{n+\frac{1}{2}}). \tag{3.6}$$

In order to better understand this scheme, by plugging (3.1) into (3.2) and (3.4) into (3.5), respectively, we can get

$$\frac{2}{\Delta t^2}y^{n+1} - \frac{1}{2}\Delta y^{n+1} = \frac{2}{\Delta t^2}y^n + \frac{2}{\Delta t}\omega^n + \frac{1}{2}\Delta y^n + \hat{q}^{n+\frac{1}{2}} f(\hat{y}^{n+\frac{1}{2}}), \tag{3.7}$$

$$\frac{4}{\Delta t^2}\hat{y}^{n+\frac{1}{2}} - \Delta\hat{y}^{n+\frac{1}{2}} = \frac{4}{\Delta t^2}y^n + \frac{2}{\Delta t}\omega^n + q^n f(y^n). \tag{3.8}$$

So we can implement the CN-E-SAV scheme as follows:

$(i)$. *Compute* $q^n$ *from* $q^n = \frac{\exp\{r^n\}}{\exp\{\mathcal{H}_2(y^n)\}}$; $(ii)$. *Compute* $\hat{y}^{n+\frac{1}{2}}$ *from* (3.8);

$(iii)$. *Compute* $\hat{\omega}^{n+\frac{1}{2}}$ *from* (3.4); $(iv)$. *Compute* $\hat{r}^{n+\frac{1}{2}}$ *from* (3.6);

$(v)$. *Compute* $\hat{q}^{n+\frac{1}{2}}$ *from* $\hat{q}^{n+\frac{1}{2}} = \frac{\exp\{\hat{r}^{n+\frac{1}{2}}\}}{\exp\{\mathcal{H}_2(\hat{y}^{n+\frac{1}{2}})\}}$; $(vi)$. *Compute* $y^{n+1}$ *from* (3.7);

$(vii)$. *Compute* $\omega^{n+1}$ *from* (3.1); $(viii)$. *Compute* $r^{n+1}$ *from* (3.3).

### *3.1. Hamiltonian conservation*

We show the conservation of the CN-E-SAV scheme by the following theorem:

**Theorem 3.1.** *The CN-E-SAV scheme* (3.1)–(3.3) *is Hamiltonian conserved:*

$$\mathcal{H}^{n+1} = \mathcal{H}^n \quad with \quad \mathcal{H}^n = \frac{1}{2}\|\omega^n\|^2 + \frac{1}{2}\|\nabla y^n\|^2 + r^n. \tag{3.9}$$

*Proof.* Taking the inner product with (3.1) and (3.2) by $y^{n+\frac{1}{2}}$, $\omega^{n+\frac{1}{2}}$, we have

$$(\omega^{n+\frac{1}{2}}, y^{n+\frac{1}{2}}) = \frac{1}{2\Delta t}\|y^{n+1}\|^2 - \frac{1}{2\Delta t}\|y^n\|^2, \tag{3.10}$$

and

$$\frac{1}{2}\|\omega^{n+1}\|^2 - \frac{1}{2}\|\omega^n\|^2 + \Delta t(\nabla y^{n+\frac{1}{2}}, \nabla\omega^{n+\frac{1}{2}}) - \hat{q}^{n+\frac{1}{2}}(f(\hat{y}^{n+\frac{1}{2}}), \omega^{n+\frac{1}{2}})\Delta t = 0. \tag{3.11}$$

Substituting (3.10) into (3.11) and combining (3.3), we obtain

$$(\frac{1}{2}\|\omega^{n+1}\|^2 + \frac{1}{2}\|\nabla y^{n+1}\|^2 + r^{n+1}) - (\frac{1}{2}\|\omega^n\|^2 + \frac{1}{2}\|\nabla y^n\|^2 + r^n) = 0.$$

The proof is complete.

### 3.2. The error of the CN-E-SAV scheme

We will follow the next two steps to complete the error estimation of the CN-E-SAV scheme:
**step (i)**: complete the error between (2.10)–(2.14) and (3.4)–(3.6);
**step (ii)**: with the help of the results of step (i), the error of (2.10)–(2.14) and (3.1)–(3.3) is further estimated.

For simplicity, we define

$$\begin{aligned} \hat{e}_\omega^{n+\frac{1}{2}} &= \omega(t_{n+\frac{1}{2}}) - \hat{\omega}^{n+\frac{1}{2}}, \qquad e_\omega^n = \omega(t_n) - \omega^n, \\ \hat{e}_y^{n+\frac{1}{2}} &= y(t_{n+\frac{1}{2}}) - \hat{y}^{n+\frac{1}{2}}, \qquad e_y^n = y(t_n) - y^n, \\ \hat{e}_r^{n+\frac{1}{2}} &= r(t_{n+\frac{1}{2}}) - \hat{r}^{n+\frac{1}{2}}, \qquad e_r^n = r(t_n) - r^n. \end{aligned}$$

It follows from (2.10)–(2.14) that the exact solution $(\omega, y, r)$ satisfies

$$\omega(t_{n+\frac{1}{2}}) = \frac{1}{\Delta t/2}(y(t_{n+\frac{1}{2}}) - y(t_n)) - \frac{1}{\Delta t/2}\hat{\mathcal{T}}_{y_1}^n, \tag{3.12}$$

$$\frac{\omega(t_{n+\frac{1}{2}}) - \omega(t_n)}{\Delta t/2} - \Delta y(t_{n+\frac{1}{2}}) - q(t_n)f(y(t_n)) = \frac{1}{\Delta t/2}\hat{\mathcal{T}}_\omega^n - \Delta(y(t_{n+\frac{1}{2}}) - y(t_n)), \tag{3.13}$$

$$r(t_{n+\frac{1}{2}}) - r(t_n) = -(q(t_n)f(y(t_n)), y(t_{n+\frac{1}{2}}) - y(t_n) - \hat{\mathcal{T}}_{y_2}^n) + \hat{\mathcal{T}}_r^n, \tag{3.14}$$

where the truncation functions are defined as

$$\begin{aligned} \hat{\mathcal{T}}_\omega^n &= \int_{t_n}^{t_{n+\frac{1}{2}}} (t_{n+\frac{1}{2}} - t)\omega_{tt}dt, \quad \hat{\mathcal{T}}_{y_1}^n = \int_{t_n}^{t_{n+\frac{1}{2}}} (t_n - t)y_{tt}dt, \\ \hat{\mathcal{T}}_{y_2}^n &= \int_{t_n}^{t_{n+\frac{1}{2}}} (t_{n+\frac{1}{2}} - t)y_{tt}dt, \quad \hat{\mathcal{T}}_r^n = \int_{t_n}^{t_{n+\frac{1}{2}}} (t_{n+\frac{1}{2}} - t)r_{tt}dt, \end{aligned}$$

and satisfy

$$\|\hat{\mathcal{T}}_\omega^n\|^2 \le C(\Delta t)^3 \int_{t_n}^{t_{n+\frac{1}{2}}} \|\omega_{tt}\|^2 dt, \quad \|\hat{\mathcal{T}}_{y_1}^n\|^2 \le C(\Delta t)^3 \int_{t_n}^{t_{n+\frac{1}{2}}} \|y_{tt}\|^2 dt, \tag{3.15}$$

$$\|\hat{\mathcal{T}}_{y_2}^n\|^2 \le C(\Delta t)^3 \int_{t_n}^{t_{n+\frac{1}{2}}} \|y_{tt}\|^2 dt, \quad |\hat{\mathcal{T}}_r^n|^2 \le C(\Delta t)^3 \int_{t_n}^{t_{n+\frac{1}{2}}} |r_{tt}|^2 dt. \tag{3.16}$$

For the purposes of theorem proving, we present the following assumptions and lemmas:

**Assumption 3.1.** *There exist constants $Q^*$, $Q_*$, $\tilde{Q}^*$, and $\tilde{Q}_*$ independent of $\Delta t$ such that $Q_* \le q^n \le Q^*$, $\tilde{Q}_* \le \hat{q}^{n+\frac{1}{2}} \le \tilde{Q}^*$ for all n.*

**Lemma 3.1.** *Denote*

$$\begin{aligned} \mathcal{A} &= q(t_n)f(y(t_n)) - q^n f(y^n), \\ \mathcal{B} &= \hat{q}^{n+\frac{1}{2}} f(\hat{y}^{n+\frac{1}{2}}) - q(t_{n+\frac{1}{2}})f(y(t_{n+\frac{1}{2}})), \end{aligned}$$

*then the following holds:*

$$\begin{aligned} \|\mathcal{A}\| &\le C(\|\nabla e_y^n\| + |e_r^n|), \\ \|\mathcal{B}\| &\le C(\|\nabla \hat{e}_y^{n+\frac{1}{2}}\| + |\hat{e}_r^{n+\frac{1}{2}}|), \end{aligned}$$

*where the constant $C > 0$ depends on $Q^*, Q_*, \tilde{Q}^*, \tilde{Q}_*, |\Omega|, y_0,$ and $\|f\|_{C^1(R)}$.*

*Proof.* Similar to the proof of Lemma 4 of [51], the results can be proved by applying Poincaré's inequality to $\|e_y^n\|, \|\hat{e}_y^{n+\frac{1}{2}}\|$ once more.

**Lemma 3.2.** *Assume $\Delta t$ is sufficiently small and satisfies*

$$y_t \in L^\infty(0,T;L^2) \cap L^2(0,T;H^2), y_{tt} \in L^2(0,T;L^2) \cap L^2(0,T;H^1), y_{ttt} \in L^2(0,T;L^2).$$

*Then, we have*

$$\begin{aligned}
&\|\hat{e}_\omega^{n+\frac{1}{2}}\|^2 + \|\nabla \hat{e}_y^{n+\frac{1}{2}}\|^2 + |\hat{e}_r^{n+\frac{1}{2}}|^2 \\
\leq &\check{C}(\Delta t)^3 \int_{t_n}^{t_{n+\frac{1}{2}}} (\|\omega_{tt}\|^2 + \|\nabla y_{tt}\|^2 + |r_{tt}|^2 + \|y_{tt}\|^2 + \|y_t\|^2_{H^2(\Omega)}) ds \\
&+ \check{C}(\|e_\omega^n\|^2 + \|\nabla e_y^n\|^2 + |e_r^n|^2).
\end{aligned} \tag{3.17}$$

*Proof.* Subtracting (3.4)–(3.6) from (3.12)–(3.14), we have the error equations as

$$\hat{e}_\omega^{n+\frac{1}{2}} = \frac{1}{\Delta t/2}(\hat{e}_y^{n+\frac{1}{2}} - e_y^n) - \frac{1}{\Delta t/2}\hat{\mathcal{T}}_{y_1}^n, \tag{3.18}$$

$$\frac{\hat{e}_\omega^{n+\frac{1}{2}} - e_\omega^n}{\Delta t/2} - \Delta \hat{e}_y^{n+\frac{1}{2}} = q(t_n)f(y(t_n)) - q^n f(y^n) - \Delta(y(t_{n+\frac{1}{2}}) - y(t_n)) + \frac{1}{\Delta t/2}\hat{\mathcal{T}}_\omega^n, \tag{3.19}$$

$$\begin{aligned}
\hat{e}_r^{n+\frac{1}{2}} - e_r^n = &-\left(q^n f(y^n), \hat{e}_y^{n+\frac{1}{2}} - e_y^n\right) + \left(q^n f(y^n) - q(t_n)f(y(t_n)), y(t_{n+\frac{1}{2}}) - y(t_n)\right) \\
&+ (q(t_n)f(y(t_n)), \hat{\mathcal{T}}_{y_2}^n) + \hat{\mathcal{T}}_r^n.
\end{aligned} \tag{3.20}$$

Taking the inner product of (3.19) with $\hat{e}_\omega^{n+\frac{1}{2}}$ and combining (3.18), we have

$$\begin{aligned}
&\|\hat{e}_\omega^{n+\frac{1}{2}}\|^2 - \|e_\omega^n\|^2 + \|\hat{e}_\omega^{n+\frac{1}{2}} - e_\omega^n\|^2 \\
&+ \|\nabla \hat{e}_y^{n+\frac{1}{2}}\|^2 - \|\nabla e_y^n\|^2 + \|\nabla(\hat{e}_y^{n+\frac{1}{2}} - e_y^n)\|^2 \\
=&\Delta t(\mathcal{A}, \hat{e}_\omega^{n+\frac{1}{2}}) - \Delta t(\Delta(y(t_{n+\frac{1}{2}}) - y(t_n)), \hat{e}_\omega^{n+\frac{1}{2}}) \\
&+ 2(\hat{\mathcal{T}}_\omega^n, \hat{e}_\omega^{n+\frac{1}{2}}) - 2(\hat{\mathcal{T}}_{y_1}^n, \Delta \hat{e}_y^{n+\frac{1}{2}}) \\
:=&\Lambda_1 + \Lambda_2 + \Lambda_3 + \Lambda_4.
\end{aligned} \tag{3.21}$$

For the first term on the right-hand side of (3.21), according to Lemma 3.1, we obtain

$$\begin{aligned}
\Lambda_1 \leq &C(\Delta t)^2\|\mathcal{A}\|^2 + \frac{1}{4}\|\hat{e}_\omega^{n+\frac{1}{2}}\|^2 \\
\leq &\tilde{C}_1(\Delta t)^2(\|\nabla e_y^n\|^2 + |e_r^n|^2) + \frac{1}{4}\|\hat{e}_\omega^{n+\frac{1}{2}}\|^2.
\end{aligned} \tag{3.22}$$

Then for $\Lambda_2,\ \Lambda_3,\ \Lambda_4$ , using Young's inequality and (3.15), one has

$$\Lambda_2 \leq C(\Delta t)^3 \int_{t_n}^{t_{n+\frac{1}{2}}} \|y_t\|^2_{H^2(\Omega)} ds + \frac{1}{4}\|\hat{e}_\omega^{n+\frac{1}{2}}\|^2, \tag{3.23}$$

$$\Lambda_3 \leq C(\Delta t)^3 \int_{t_n}^{t_{n+\frac{1}{2}}} \|\omega_{tt}\|^2 dt + \frac{1}{4}\|\hat{e}_\omega^{n+\frac{1}{2}}\|^2, \tag{3.24}$$

$$\Lambda_4 \leq C(\Delta t)^3 \int_{t_n}^{t_{n+\frac{1}{2}}} \|\nabla y_{tt}\|^2 dt + \frac{1}{4}\|\nabla \hat{e}_y^{n+\frac{1}{2}}\|^2. \tag{3.25}$$

Combining (3.22)–(3.25) with (3.21), we can have

$$\begin{aligned}
&\|\hat{e}_\omega^{n+\frac{1}{2}}\|^2 + 4\|\hat{e}_\omega^{n+\frac{1}{2}} - e_\omega^n\|^2 + \|\nabla \hat{e}_y^{n+\frac{1}{2}}\|^2 + 4\|\nabla(\hat{e}_y^{n+\frac{1}{2}} - e_y^n)\|^2 \\
\leq & 4\tilde{C}_1(\Delta t)^2(\|\nabla e_y^n\|^2 + |e_r^n|^2) + 4(\|e_\omega^n\|^2 + \|\nabla e_y^n\|^2) \\
&+ C(\Delta t)^3 \int_{t_n}^{t_{n+\frac{1}{2}}} (\|\omega_{tt}\|^2 + \|\nabla y_{tt}\|^2 + \|y_t\|^2_{H^2(\Omega)}) ds.
\end{aligned} \tag{3.26}$$

Multiplying (3.20) by $\hat{e}_r^{n+\frac{1}{2}}$, we can obtain

$$\begin{aligned}
&|\hat{e}_r^{n+\frac{1}{2}}|^2 - |e_r^n|^2 + |\hat{e}_r^{n+\frac{1}{2}} - e_r^n|^2 \\
= & -2(q^n f(y^n), \hat{e}_y^{n+\frac{1}{2}} - e_y^n)\hat{e}_r^{n+\frac{1}{2}} - 2(\mathcal{A}, y(t_{n+\frac{1}{2}}) - y(t_n))\hat{e}_r^{n+\frac{1}{2}} \\
&+ 2(q(t_n) f(y(t_n)), \hat{\mathcal{T}}_{y_2}^n)\hat{e}_r^{n+\frac{1}{2}} + 2\hat{\mathcal{T}}_r^n \hat{e}_r^{n+\frac{1}{2}} \\
:= & \Psi_1 + \Psi_2 + \Psi_3 + \Psi_4.
\end{aligned} \tag{3.27}$$

According to $q^n \leq Q^*$, $F \in C^3(R)$, and Poincaré's inequality, we can derive the following estimate for $\Psi_1$:

$$\begin{aligned}
\Psi_1 &\leq \|q^n f(y^n)\| \|\hat{e}_y^{n+\frac{1}{2}} - e_y^n\| |\hat{e}_r^{n+\frac{1}{2}}| \\
&\leq C^* \|\nabla(\hat{e}_y^{n+\frac{1}{2}} - e_y^n)\|^2 + \frac{1}{4}|\hat{e}_r^{n+\frac{1}{2}}|^2.
\end{aligned} \tag{3.28}$$

The estimate for $\Psi_2$ is similar to (3.22), so we obtain

$$\begin{aligned}
\Psi_2 &\leq \Delta t \|\mathcal{A}\| \left\| \frac{y(t_{n+\frac{1}{2}}) - y(t_n)}{\Delta t} \right\| |\hat{e}_r^{n+\frac{1}{2}}| \\
&\leq \tilde{C}_2(\Delta t)^2(\|\nabla e_y^n\|^2 + |e_r^n|^2) + \frac{1}{4}|\hat{e}_r^{n+\frac{1}{2}}|^2.
\end{aligned} \tag{3.29}$$

For the last two terms of (3.27), by utilizing (3.16), we have that

$$\Psi_3 + \Psi_4 \leq C(\Delta t)^3 \int_{t_n}^{t_{n+\frac{1}{2}}} (|r_{tt}|^2 + \|y_{tt}\|^2) ds + \frac{1}{4}|\hat{e}_r^{n+\frac{1}{2}}|^2. \tag{3.30}$$

Therefore, injecting (3.28)–(3.30) into (3.27) leads to

$$\begin{aligned}
&|\hat{e}_r^{n+\frac{1}{2}}|^2 + 4|\hat{e}_r^{n+\frac{1}{2}} - e_r^n|^2 \\
\leq & 4\tilde{C}_2(\Delta t)^2(\|\nabla e_y^n\|^2 + |e_r^n|^2) + C(\Delta t)^3 \int_{t_n}^{t_{n+\frac{1}{2}}} (|r_{tt}|^2 + \|y_{tt}\|^2) dt \\
&+ 4C^* \|\nabla(\hat{e}_y^{n+\frac{1}{2}} - e_y^n)\|^2 + 4|e_r^n|^2.
\end{aligned} \tag{3.31}$$

Multiplying (3.26) by $C^*$ and adding it to (3.31) implies

$$\begin{aligned}&C^*\|\hat{e}_\omega^{n+\frac{1}{2}}\|^2+C^*\|\nabla\hat{e}_y^{n+\frac{1}{2}}\|^2+|\hat{e}_r^{n+\frac{1}{2}}|^2\\ \leq&4(\tilde{C}_1C^*+\tilde{C}_2)(\Delta t)^2(\|\nabla e_y^n\|^2+|e_r^n|^2)+4C^*(\|e_\omega^n\|^2+\|\nabla e_y^n\|^2)+4|e_r^n|^2\\ &+C(\Delta t)^3\int_{t_n}^{t_{n+\frac{1}{2}}}(\|\omega_{tt}\|^2+\|\nabla y_{tt}\|^2+|r_{tt}|^2+\|y_{tt}\|^2+\|y_t\|^2_{H^2(\Omega)})ds.\end{aligned}$$

The proof is completed when $C^*\geq 1$ and $(\Delta t)^2\leq\frac{C^*}{\tilde{C}_1C^*+\tilde{C}_2}$.

Next, we will derive the convergence order of the CN-E-SAV scheme (3.1)–(3.3). Clearly, the exact solution $(\omega, y, r)$ satisfies

$$\frac{\omega(t_{n+1})+\omega(t_n)}{2}=\frac{1}{\Delta t}(y(t_{n+1})-y(t_n))+\mathcal{R}_\omega^n-\frac{1}{\Delta t}\mathcal{T}_y^n, \tag{3.32}$$

$$\frac{1}{\Delta t}(\omega(t_{n+1})-\omega(t_n))-\Delta\frac{y(t_{n+1})+y(t_n)}{2}-q(t_{n+\frac{1}{2}})f(y(t_{n+\frac{1}{2}}))=\frac{1}{\Delta t}\mathcal{T}_\omega^n-\Delta\mathcal{R}_y^n, \tag{3.33}$$

$$\frac{1}{\Delta t}(r(t_{n+1})-r(t_n))=-\left(q(t_{n+\frac{1}{2}})f(y(t_{n+\frac{1}{2}})),\frac{\omega(t_{n+1})+\omega(t_n)}{2}-\mathcal{R}_\omega\right)+\frac{1}{\Delta t}\mathcal{T}_r^n, \tag{3.34}$$

where the truncation functions are defined by

$$\begin{aligned}&\mathcal{T}_\omega=\omega(t_{n+1})-\omega(t_n)-\Delta t\omega_t(t_{n+\frac{1}{2}}), && \mathcal{T}_y=y(t_{n+1})-y(t_n)-\Delta ty_t(t_{n+\frac{1}{2}}),\\ &\mathcal{T}_r=r(t_{n+1})-r(t_n)-\Delta tr_t(t_{n+\frac{1}{2}}), && \mathcal{R}_\omega=\frac{\omega(t_{n+1})+\omega(t_n)}{2}-\omega(t_{n+\frac{1}{2}}),\\ &\mathcal{R}_y=\frac{y(t_{n+1})+y(t_n)}{2}-y(t_{n+\frac{1}{2}}), && \mathcal{R}_r=\frac{r(t_{n+1})+r(t_n)}{2}-r(t_{n+\frac{1}{2}}).\end{aligned}$$

The truncation functions satisfy the following lemma:

**Lemma 3.3.** *( [50]) The following estimates hold*

$$\begin{aligned}&\|\mathcal{T}_\omega\|^2\leq C(\Delta t)^5\int_{t_n}^{t_{n+1}}\|\omega_{ttt}\|^2ds, && \|\mathcal{T}_y\|^2\leq C(\Delta t)^5\int_{t_n}^{t_{n+1}}\|y_{ttt}\|^2ds,\\ &|\mathcal{T}_r|^2\leq C(\Delta t)^5\int_{t_n}^{t_{n+1}}|r_{ttt}|^2ds, && \|\mathcal{R}_\omega\|^2\leq C(\Delta t)^3\int_{t_n}^{t_{n+1}}\|\omega_{tt}\|^2ds,\\ &\|\mathcal{R}_y\|^2\leq C(\Delta t)^3\int_{t_n}^{t_{n+1}}\|y_{tt}\|^2ds, && |\mathcal{R}_r|^2\leq C(\Delta t)^3\int_{t_n}^{t_{n+1}}|r_{tt}|^2ds.\end{aligned}$$

**Theorem 3.2.** *Let* $(\omega(t_n), y(t_n), r(t_n))$ *and* $(\omega^n, y^n, r^n)$ *be the solutions of* (2.10)–(2.14) *and CN-E-SAV scheme* (3.1)–(3.3)*, respectively. Suppose that the assumptions in Lemma 3.2 hold and assume further*

$$y_{tt}\in L^2(0,T;L^2)\cap L^2(0,T;H^2), y_{ttt}\in L^2(0,T;L^2)\cap L^2(0,T;H^1), y_{tttt}\in L^2(0,T;L^2).$$

*Then, we have*

$$\|e_\omega^n\|^2+\|\nabla e_y^n\|^2+|e_r^n|^2\leq C(\Delta t)^4.$$

*Proof.* Subtracting (3.1)–(3.3) from (3.32)–(3.34), we derive the following error equations:

$$e_\omega^{n+\frac{1}{2}} = \frac{1}{\Delta t}(e_y^{n+1} - e_y^n) + \mathcal{R}_\omega^n - \frac{1}{\Delta t}\mathcal{T}_y^n, \tag{3.35}$$

$$\frac{1}{\Delta t}(e_\omega^{n+1} - e_\omega^n) - \Delta e_y^{n+\frac{1}{2}} = q(t_{n+\frac{1}{2}})f(y(t_{n+\frac{1}{2}})) - \hat{q}^{n+\frac{1}{2}}f(\hat{y}^{n+\frac{1}{2}}) + \frac{1}{\Delta t}\mathcal{T}_\omega^n - \Delta\mathcal{R}_y^n, \tag{3.36}$$

$$\begin{aligned}\frac{1}{\Delta t}(e_r^{n+1} - e_r^n) = &\left(\hat{q}^{n+\frac{1}{2}}f(\hat{y}^{n+\frac{1}{2}}) - q(t_{n+\frac{1}{2}})f(y(t_{n+\frac{1}{2}})), \frac{\omega(t_{n+1}) + \omega(t_n)}{2}\right)\\ &- (\hat{q}^{n+\frac{1}{2}}f(\hat{y}^{n+\frac{1}{2}}), e_\omega^{n+\frac{1}{2}}) + (q(t_{n+\frac{1}{2}})f(y(t_{n+\frac{1}{2}})), \mathcal{R}_\omega^n) + \frac{1}{\Delta t}\mathcal{T}_r^n.\end{aligned} \tag{3.37}$$

Taking the inner product of (3.36) with $e_\omega^{n+\frac{1}{2}}$ and combining (3.35), we have

$$\begin{aligned}&\frac{1}{2}\|e_\omega^{n+1}\|^2 - \frac{1}{2}\|e_\omega^n\|^2 + \frac{1}{2}\|\nabla e_y^{n+1}\|^2 - \frac{1}{2}\|\nabla e_y^n\|^2\\ =& - \Delta t(\mathcal{B}, e_\omega^{n+\frac{1}{2}}) + (\mathcal{T}_\omega^n, e_\omega^{n+\frac{1}{2}}) - \Delta t(\Delta\mathcal{R}_y^n, e_\omega^{n+\frac{1}{2}})\\ &- \Delta t(\nabla e_y^{n+\frac{1}{2}}, \nabla\mathcal{R}_\omega^n) - \Delta t(\nabla e_y^{n+\frac{1}{2}}, \nabla\mathcal{T}_y^n)\\ :=&\Upsilon_1 + \Upsilon_2 + \Upsilon_3 + \Upsilon_4 + \Upsilon_5.\end{aligned} \tag{3.38}$$

According to Lemma 3.1, we obtain

$$\Upsilon_1 \leq C\Delta t(|\hat{e}_r^{n+\frac{1}{2}}|^2 + \|\nabla\hat{e}_y^{n+\frac{1}{2}}\|^2 + \|e_\omega^{n+\frac{1}{2}}\|^2). \tag{3.39}$$

For the last four terms of (3.38), it follows from Lemma 3.3 that

$$\Upsilon_2 \leq C(\Delta t)^4\int_{t_n}^{t_{n+1}}\|\omega_{ttt}\|^2dt + C\Delta t\|e_\omega^{n+\frac{1}{2}}\|^2, \tag{3.40}$$

$$\Upsilon_3 \leq C(\Delta t)^4\int_{t_n}^{t_{n+1}}\|\Delta y_{tt}\|^2dt + C\Delta t\|e_\omega^{n+\frac{1}{2}}\|^2, \tag{3.41}$$

$$\Upsilon_4 \leq C(\Delta t)^4\int_{t_n}^{t_{n+1}}\|\nabla\omega_{tt}\|^2dt + C\Delta t\|\nabla e_y^{n+\frac{1}{2}}\|^2, \tag{3.42}$$

$$\Upsilon_5 \leq C(\Delta t)^4\int_{t_n}^{t_{n+1}}\|\nabla y_{ttt}\|^2dt + C\Delta t\|\nabla e_y^{n+\frac{1}{2}}\|^2. \tag{3.43}$$

Substituting (3.39)–(3.43) into (3.38), we can obtain

$$\begin{aligned}&\frac{1}{2}\|e_\omega^{n+1}\|^2 - \frac{1}{2}\|e_\omega^n\|^2 + \frac{1}{2}\|\nabla e_y^{n+1}\|^2 - \frac{1}{2}\|\nabla e_y^n\|^2\\ \leq& C\Delta t(|\hat{e}_r^{n+\frac{1}{2}}|^2 + \|\nabla\hat{e}_y^{n+\frac{1}{2}}\|^2) + C\Delta t(\|e_\omega^{n+\frac{1}{2}}\|^2 + \|\nabla e_y^{n+\frac{1}{2}}\|^2)\\ &+ C(\Delta t)^4\int_{t_n}^{t_{n+1}}\left(\|\omega_{ttt}\|^2 + \|\nabla y_{ttt}\|^2 + \|\Delta y_{tt}\|^2 + \|\nabla\omega_{tt}\|^2\right)dt.\end{aligned} \tag{3.44}$$

Multiplying (3.3) by $e_r^{n+\frac{1}{2}}$, we obtain

$$\frac{1}{2}(|e_r^{n+1}|^2 - |e_r^n|^2)$$

$$
\begin{aligned}
&=\Delta t e_r^{n+\frac{1}{2}}\left(\mathcal{B}, \frac{\omega(t_{n+1})+\omega(t_n)}{2}\right)-\Delta t e_r^{n+\frac{1}{2}}(\hat{q}^{n+\frac{1}{2}} f(\hat{y}^{n+\frac{1}{2}}), e_\omega^{n+\frac{1}{2}}) \\
&\quad+\Delta t(q(t_{n+\frac{1}{2}}) f(y(t_{n+\frac{1}{2}})), \mathcal{R}_\omega^n) e_r^{n+\frac{1}{2}}+\mathcal{T}_r^n e_r^{n+\frac{1}{2}} \\
&:=\Phi_1+\Phi_2+\Phi_3+\Phi_4. \qquad (3.45)
\end{aligned}
$$

Next, we estimate the right-hand side of (3.45). Applying Lemma 3.1, Lemma 3.3, and Young's inequality, we deduce that

$$
\begin{aligned}
\Phi_1 &\leq C\Delta t|e_r^{n+\frac{1}{2}}|\|\mathcal{B}\|\|\frac{\omega(t_{n+1})+\omega(t_n)}{2}\| \\
&\leq C\Delta t(|\hat{e}_r^{n+\frac{1}{2}}|^2+\|\nabla \hat{e}_y^{n+\frac{1}{2}}\|^2+|e_r^{n+\frac{1}{2}}|^2), \qquad (3.46)\\
\Phi_2 &\leq C\Delta t(|e_r^{n+\frac{1}{2}}|^2+\|e_\omega^{n+\frac{1}{2}}\|^2), \qquad (3.47)\\
\Phi_3+\Phi_4 &\leq C(\Delta t)^4\int_{t_n}^{t_{n+1}}(\|\omega_{tt}\|^2+|r_{ttt}|^2)dt+C\Delta t|e_r^{n+\frac{1}{2}}|^2. \qquad (3.48)
\end{aligned}
$$

Combining the above estimates of (3.46)–(3.48) together, one has

$$
\begin{aligned}
&\frac{1}{2}|e_r^{n+1}|^2-\frac{1}{2}|e_r^n|^2 \\
\leq& C\Delta t(|\hat{e}_r^{n+\frac{1}{2}}|^2+\|\nabla \hat{e}_y^{n+\frac{1}{2}}\|^2)+C\Delta t(\|e_\omega^{n+\frac{1}{2}}\|^2+|e_r^{n+\frac{1}{2}}|^2) \\
&+C(\Delta t)^4\int_{t_n}^{t_{n+1}}(\|\omega_{tt}\|^2+|r_{ttt}|^2)dt. \qquad (3.49)
\end{aligned}
$$

By adding (3.44) and (3.49) and summing the index $k$ from 0 to $n-1$, we obtain

$$
\begin{aligned}
&\|e_\omega^n\|^2+\|\nabla e_y^n\|^2+\|e_r^n\|^2 \\
\leq& C\Delta t\sum_{k=0}^{n-1}(\|e_\omega^k\|^2+\|\nabla e_y^k\|^2+|e_r^k|^2)+C\Delta t\sum_{k=0}^{n-1}(|\hat{e}_r^{k+\frac{1}{2}}|^2+\|\nabla \hat{e}_y^{k+\frac{1}{2}}\|^2) \\
&+C(\Delta t)^4\int_0^{t_n}(\|\omega_{ttt}\|^2+|r_{ttt}|^2+\|\nabla y_{ttt}\|^2 \\
&\qquad+\|\omega_{tt}\|^2+\|y_{tt}\|^2+|r_{tt}|^2+\|\Delta y_{tt}\|^2+\|\nabla \omega_{tt}\|^2)dt.
\end{aligned}
$$

Applying Lemma 3.2 and the discrete Gronwall's inequality, we can complete the proof.

## 4. New-CN-E-SAV scheme

For the system (2.18)–(2.24), we obtain the semi-discrete new Crank−Nicolson E-SAV ( **New-CN-E-SAV**) scheme by adopting the Crank−Nicolson scheme as

$$
\frac{\omega^{n+1}+\omega^n}{2}=\frac{1}{\Delta t}(y^{n+1}-y^n), \qquad (4.1)
$$

$$
\frac{1}{\Delta t}(\omega^{n+1}-\omega^n)-\Delta\frac{y^{n+1}+y^n}{2}-Q(\xi^{n+1})f(\hat{y}^{n+\frac{1}{2}})=0, \qquad (4.2)
$$

$$\xi^{n+1} = \frac{\exp(\mathcal{R}^{n+1})}{\exp(H(\hat{y}^{n+\frac{1}{2}}))}, \tag{4.3}$$

$$Q(\xi^{n+1}) = \xi^{n+1}(2 - \xi^{n+1}), \tag{4.4}$$

$$\frac{1}{\Delta t}(\mathcal{R}^{n+1} - \mathcal{R}^n) = 0, \tag{4.5}$$

where $\hat{y}^{n+\frac{1}{2}}$ is obtained by solving the following equation:

$$\hat{w}^{n+\frac{1}{2}} = \frac{1}{\Delta t/2}(\hat{y}^{n+\frac{1}{2}} - y^n), \tag{4.6}$$

$$\frac{1}{\Delta t/2}(\hat{\omega}^{n+\frac{1}{2}} - \omega^n) - \Delta\hat{y}^{n+\frac{1}{2}} - f(y^n) = 0. \tag{4.7}$$

From (4.5), we can find that the New-CN-E-SAV scheme (4.1)–(4.5) also enjoys the same conservation as the CN-E-SAV scheme (3.1)–(3.3).

**Theorem 4.1.** *The New-CN-E-SAV scheme* (4.1)–(4.5) *is Hamiltonian conserved in the sense that*

$$\mathcal{R}^{n+1} = \mathcal{R}^n = \cdots = \mathcal{R}^0.$$

Further, according to Theorem 4.1, the Eq (4.3) can be simplified as

$$\xi^{n+1} = \frac{\exp(\mathcal{R}^0)}{\exp(H(\hat{y}^{n+\frac{1}{2}}))}. \tag{4.8}$$

In order to better illustrate the calculation process of the New-CN-E-SAV scheme (4.1)–(4.5), plugging (4.1) and (4.6) into (4.2) and (4.7), respectively, we obtain

$$(\frac{2}{\Delta t^2} - \frac{1}{2}\Delta)y^{n+1} = \frac{2}{\Delta t^2}y^n + \frac{2}{\Delta t}\omega^n + \frac{1}{2}\Delta y^n + Q(\xi^{n+1})f(\hat{y}^{n+\frac{1}{2}}), \tag{4.9}$$

$$(\frac{4}{\Delta t^2} - \Delta)\hat{y}^{n+\frac{1}{2}} = \frac{4}{\Delta t^2}y^n + \frac{2}{\Delta t}\omega^n + f(y^n). \tag{4.10}$$

So the New-CN-E-SAV scheme can be implemented as follows:

$$(i).\ \ solve\ \hat{y}^{n+\frac{1}{2}}\ from\ (4.10); \qquad (ii).\ \ solve\ \hat{\omega}^{n+\frac{1}{2}}\ from\ (4.6);$$
$$(iii).\ \ compute\ \xi^{n+1}\ from\ (4.8); \qquad (iv).\ \ compute\ Q(\xi^{n+1})\ from\ (4.4);$$
$$(v).\ \ solve\ y^{n+\frac{1}{2}}\ from\ (4.9); \qquad (vi).\ \ solve\ \omega^{n+\frac{1}{2}}\ from\ (4.1).$$

For the convergence order of the New-CN-E-SAV scheme, from (4.6) and (4.7), we can obtain

$$\hat{y}^{n+\frac{1}{2}} = y(t^{n+\frac{1}{2}}) + O(\Delta t^2), \tag{4.11}$$

$$\hat{\omega}^{n+\frac{1}{2}} = \omega(t^{n+\frac{1}{2}}) + O(\Delta t^2). \tag{4.12}$$

Referring to [46] and combining (4.11) and (4.12), we obtain

$$\xi^{n+1} = \frac{\exp(\mathcal{R}^0)}{\exp(H(\hat{y}^{n+\frac{1}{2}}))} = \xi(t^{n+1}) + C\Delta t = 1 + C\Delta t.$$

Then, we derive that

$$\begin{aligned} Q(\xi^{n+1}) = \xi^{n+1}(2-\xi^{n+1}) &= (\xi(t^{n+1}) + C\Delta t)(2 - \xi(t^{n+1}) - C\Delta t) \\ &= (1 + C\Delta t)(1 - C\Delta t) \\ &= 1 - C^2\Delta t^2, \end{aligned}$$

which means that the New-CN-E-SAV scheme can achieve second-order approximation.

## 5. Numerical experiments

In this section, two examples are presented to test the validity of the theory. We set

$$\Omega = [0, L]^2, \ L = 2, \ T = 1,$$

$$y_0 = 0.005 \sin \pi x_1 \sin \pi x_2,$$

$$\omega_0 = 0.005 \sin \pi x_1 \sin \pi x_2,$$

and consider different nonlinear functions $F(y)$ to simulate the order of convergence and the Hamiltonian conservation. Discretize the physical space by the Fourier spectral method with a spatial step $h = L/2^9$. Since we do not have the exact solution, we thus select the sufficiently small time step $\Delta t = 1/1024$ as the reference solution.

**Example 5.1.** *In this example, we choose the nonlinear function $F(y)$ and initial values $r_0, \mathcal{R}_0$ as follows:*

$$F(y) = 1 - \cos y, \quad r_0 = \int_\Omega F(y_0) d\boldsymbol{x}, \quad \mathcal{R}_0 = H(y_0).$$

**Example 5.2.** *In this example, we select*

$$F(y) = \frac{1}{4}(y^2 - 1)^2, \quad r_0 = \int_\Omega F(y_0) d\boldsymbol{x}, \quad \mathcal{R}_0 = H(y_0).$$

For the CN-E-SAV and New-CN-E-SAV schemes, the error between the numerical solution and the exact solution in the sense of $L^2$-norm is listed in Tables 1–6, where Tables 1–3 and 4–6 show the numerical results for Examples 5.1 and 5.2, respectively.

The evolution of the Hamiltonian function with respect to the CN-E-SAV and New-CN-E-SAV schemes in Examples 5.1 and 5.2 is depicted in Figure 1.

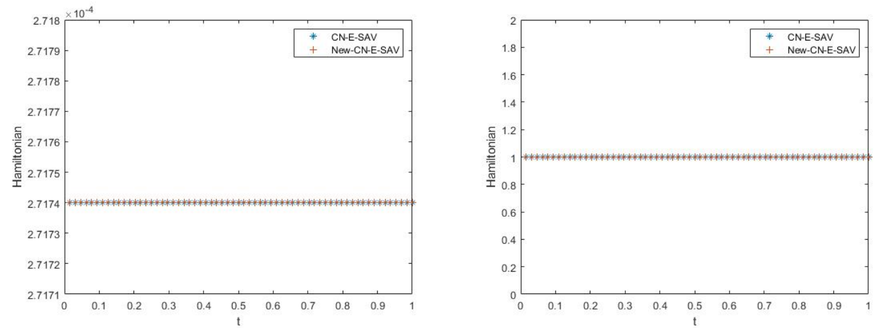


**Figure 1.** Evolutions of the Hamiltonian for the CN-E-SAV and New-CN-E-SAV schemes with the time step $\Delta t = \frac{1}{2^6}$ in Example 5.1 (left) and in Example 5.2 (right) .

**Table 1.** Error results and convergence rate of $||e_y^n||$ for the CN-E-SAV and New-CN-E-SAV schemes in Example 5.1.

| | $\Delta t$ | $\|\|e_y^n\|\|$ | Rate |
|---|---|---|---|
| CN-E-SAV | $1/2^4$ | 0.0368091884426225 | - |
| | $1/2^5$ | 0.00932236109731148 | 1.98129864079567 |
| | $1/2^6$ | 0.00233174733113645 | 1.99928392995304 |
| | $1/2^7$ | 0.000576576259379840 | 2.01582812615784 |
| | $1/2^8$ | 0.000137310038533674 | 2.07007433221585 |
| | | $\|\|e_y^n\|\|$ | Rate |
| New-CN-E-SAV | $1/2^4$ | 0.0368091815051726 | - |
| | $1/2^5$ | 0.00932235922830067 | 1.98129865813145 |
| | $1/2^6$ | 0.00233174685298024 | 1.99928393655572 |
| | $1/2^7$ | 0.000576576140697115 | 2.01582812727880 |
| | $1/2^8$ | 0.000137310011085410 | 2.07007432364543 |

**Table 2.** Error results and convergence rate of $||e_\omega^n||$ for the CN-E-SAV and New-CN-E-SAV schemes in Example 5.1.

| | $\Delta t$ | $\|\|e_\omega^n\|\|$ | Rate |
|---|---|---|---|
| CN-E-SAV | $1/2^4$ | 0.0689301039227398 | - |
| | $1/2^5$ | 0.0168861504409056 | 2.02929371796555 |
| | $1/2^6$ | 0.00418704131563571 | 2.01183741338057 |
| | $1/2^7$ | 0.00103299161999948 | 2.01910260335564 |
| | $1/2^8$ | 0.000245854829212462 | 2.07094995184852 |
| | | $\|\|e_\omega^n\|\|$ | Rate |
| New-CN-E-SAV | $1/2^4$ | 0.0689300760782284 | - |
| | $1/2^5$ | 0.0168861432622035 | 2.02929374850860 |
| | $1/2^6$ | 0.00418703950543584 | 2.01183742378274 |
| | $1/2^7$ | 0.0010329911717826 | 2.01910260561751 |
| | $1/2^8$ | 0.000245854724513483 | 2.07094994024234 |

**Table 3.** Error results and convergence rate of $|e_r^n|$ for the CN-E-SAV scheme in Example 5.1.

| | $\Delta t$ | $\|e_r^n\|$ | Rate |
|---|---|---|---|
| CN-E-SAV | $1/2^4$ | 2.86566749793482e-07 | - |
| | $1/2^5$ | 6.97595495640488e-08 | 2.03840859427113 |
| | $1/2^6$ | 1.72124441615129e-08 | 2.01893875053861 |
| | $1/2^7$ | 4.23455884358817e-09 | 2.02316839164966 |
| | $1/2^8$ | 1.00635793461970e-09 | 2.07306815290817 |

**Table 4.** Error results and convergence rate of $||e_y^n||$ for the CN-E-SAV and New-CN-E-SAV schemes in Example 5.2.

| | $\Delta t$ | $\|\|e_y^n\|\|$ | Rate |
|---|---|---|---|
| CN-E-SAV | $1/2^4$ | 0.0371725171404962 | - |
| | $1/2^5$ | 0.00943514340320470 | 1.97812003334643 |
| | $1/2^6$ | 0.00236120638866597 | 1.99852029490610 |
| | $1/2^7$ | 0.000583930678977017 | 2.01565513477143 |
| | $1/2^8$ | 0.000139064798763014 | 2.07003983134903 |
| | | $\|\|e_y^n\|\|$ | Rate |
| New-CN-E-SAV | $1/2^4$ | 0.0371725163498753 | - |
| | $1/2^5$ | 0.00943514322606903 | 1.97812002974700 |
| | $1/2^6$ | 0.00236120634599168 | 1.99852029389485 |
| | $1/2^7$ | 0.000583930668215755 | 2.01565513528492 |
| | $1/2^8$ | 0.000139064795893768 | 2.07003983452791 |

**Table 5.** Error results and convergence rate of $||e_\omega^n||$ for the CN-E-SAV and New-CN-E-SAV schemes in Example 5.2.

| | $\Delta t$ | $\|\|e_\omega^n\|\|$ | Rate |
|---|---|---|---|
| CN-E-SAV | $1/2^4$ | 0.0818241862777186 | - |
| | $1/2^5$ | 0.0201549897717315 | 2.02139029902935 |
| | $1/2^6$ | 0.00500392653834192 | 2.01000453619864 |
| | $1/2^7$ | 0.00123483574539119 | 2.01874145867249 |
| | $1/2^8$ | 0.000293902813805396 | 2.07090807463406 |
| | | $\|\|e_\omega^n\|\|$ | Rate |
| New-CN-E-SAV | $1/2^4$ | 0.0818241821912869 | - |
| | $1/2^5$ | 0.0201549887134675 | 2.02139030272942 |
| | $1/2^6$ | 0.00500392626767036 | 2.01000453848608 |
| | $1/2^7$ | 0.00123483567363466 | 2.01874146446974 |
| | $1/2^8$ | 0.000293902792746018 | 2.07090809417398 |

**Table 6.** Error results and convergence rate of $|e_r^n|$ for the CN-E-SAV scheme in Example 5.2.

| | $\Delta t$ | $\|e_r^n\|$ | Rate |
|---|---|---|---|
| CN-E-SAV | $1/2^4$ | 3.36996122007882e-07 | - |
| | $1/2^5$ | 8.30406444718435e-08 | 2.02084244415644 |
| | $1/2^6$ | 2.05944534759084e-08 | 2.01156179910102 |
| | $1/2^7$ | 5.07805131277905e-09 | 2.01990896293877 |
| | $1/2^8$ | 1.20806775694149e-09 | 2.07157359980540 |

From the analysis of the data presented in Tables 1–6, it is evident that the error decreases as the time step $\Delta t$ decreases. And the numerical results for the convergence order of the variables $\omega, y, r$ in Examples 5.1 and 5.2 are consistent with the theoretical results. This thereby further illustrates the effectiveness of the CN-E-SAV and New-CN-E-SAV schemes.

Figure 1 clearly shows that, regardless of the different nonlinear functions selected in the two examples, the CN-E-SAV and New-CN-E-SAV schemes successfully maintain the conservation property of the Hamiltonian function.

## 6. Conclusions

In this work, we develop the CN-E-SAV and New-CN-E-SAV schemes to approximate a semilinear wave equation with the following advantages: (i) it preserves Hamiltonian conservation; (ii) it is efficient; and (iv) it is easy to implement. The further topic can also involve designing the high-order BDFk-E-SAV schemes or applying them to other nonlinear problems. It is also meaningful to consider the construction of numerical schemes for the nonlinear localized wave equations.

## Use of AI tools declaration

The authors declare they have not used Artificial Intelligence (AI) tools in the creation of this article.

## Acknowledgments

This work is supported by the National Natural Science Foundation of China (Granted No. 11961008) and Guizhou University Doctoral Foundation (Granted NO. 15 (2022)).

## Conflict of interest

The authors declare there is no conflict of interest.

## References

1. V. E. Zakharov, Exact solutions to the problem of the parametric interaction of three-dimensional wave packets, *Sov. Phys. Dokl.*, **21** (1976).

2. A. D. D. Craik, J. A. Adam, Evolution in space and time of resonant wave triads-I. The'pump-wave approximation', *Proc. R. Soc. Lond. A. Math. Phys. Sci.*, **363** (1978), 243–255. https://doi.org/10.1098/rspa.1978.0166

3. I. Ahmed, A. R. Seadawy, D. Lu, Mixed lump-solitons, periodic lump and breather soliton solutions for (2+ 1)-dimensional extended Kadomtsev-Petviashvili dynamical equation, *Int. J. Mod. Phys. B*, **33** (2019), 1950019. https://doi.org/10.1142/S021797921950019X

4. Y. L. Ma, B. Q. Li, Interactions between soliton and rogue wave for a (2+1)-dimensional generalized breaking soliton system: hidden rogue wave and hidden soliton, *Comput. Math. Appl.*, **78** (2019), 827–839. https://doi.org/10.1016/j.camwa.2019.03.002

5. A. Yusuf, T. A. Sulaiman, M. Inc, M. Bayram, Breather wave, lump-periodic solutions and some other interaction phenomena to the Caudrey-Dodd-Gibbon equation, *Eur. Phys. J. Plus*, **135** (2020), 1–8. https://doi.org/10.1140/epjp/s13360-020-00566-7

6. K. Hosseini, M. Samavat, M. Mirzazadeh, S. Salahshour, D. Baleanu, A new (4+1)-dimensional burgers equation: its backlund transformation and real and complex N-Kink solitons, *Int. J. Appl. Comput. Math.*, **8** (2022), 172. https://doi.org/10.1007/s40819-022-01359-5

7. B. Q. Li, Y. L. Ma, Multiple-lump waves for a (3+1)-dimensional Boiti-Leon-Manna-Pempinelli equation arising from incompressible fluid, *Comput. Math. Appl.*, **76** (2018), 204–214. https://doi.org/10.1016/j.camwa.2018.04.015

8. W. X. Ma, Riemann-Hilbert problems and soliton solutions of type ($-\lambda, \lambda$) reduced nonlocal integrable mKdV hierarchies, *Mathematics*, **10** (2022), 870. https://doi.org/10.3390/math10060870

9. Z. Zhao, L. He, M-lump, high-order breather solutions and interaction dynamics of a generalized (2+1)-dimensional nonlinear wave equation, *Nonlinear Dyn.*, **100** (2020), 2753–2765. https://doi.org/10.1007/s11071-020-05611-9

10. J. G. Liu, M. S. Osman, Nonlinear dynamics for different nonautonomous wave structures solutions of a 3D variable-coefficient generalized shallow water wave equation, *Chin. J. Phys.*, **77** (2022), 1618–1624. https://doi.org/10.1016/j.cjph.2021.10.026

11. U. Younas, T. A. Sulaiman, J. Ren, A. Yusuf, Lump interaction phenomena to the nonlinear ill-posed Boussinesq dynamical wave equation, *J. Geom. Phys.*, **178** (2022), 104586. https://doi.org/10.1016/j.geomphys.2022.104586

12. H. F. Ismael, H. Bulut, M. S. Osman, The N-soliton, fusion, rational and breather solutions of two extensions of the (2+1)-dimensional Bogoyavlenskii-Schieff equation, *Nonlinear Dyn.*, **107** (2022), 3791–3803. https://doi.org/10.1007/s11071-021-07154-z

13. S. Saifullah, S. Ahmad, M. A. Alyami, M. Inc, Analysis of interaction of lump solutions with kink-soliton solutions of the generalized perturbed KdV equation using Hirota bilinear approach, *Phys. Lett. A*, **454** (2022), 128503. https://doi.org/10.1016/j.physleta.2022.128503

14. Q. J. Feng, G. Q. Zhang, Lump solution, lump-stripe solution, rogue wave solution and periodic solution of the (2+1)-dimensional Fokas system, *Nonlinear Dyn.*, **112** (2024), 4775–4792. https://doi.org/10.1007/s11071-023-09243-7

15. A. Degasperis, S. Lombardo, M. Sommacal, Integrability and linear stability of nonlinear waves, *J. Nonlinear Sci.*, **28** (2018), 1251–1291. https://doi.org/10.1007/s00332-018-9450-5

16. M. J. Ablowitz, Integrability and nonlinear waves, *Emerging Front. Nonlinear Sci.*, **32** (2020), 161–184. https://doi.org/10.1007/978-3-030-44992-6_7

17. M. He, P. Sun, Energy-preserving finite element methods for a class of nonlinear wave equations, *Appl. Numer. Math.*, **157** (2020), 446–469. https://doi.org/10.1016/j.apnum.2020.06.016

18. M. He, J. Tian, P. Sun, Z. Zhang, An energy-conserving finite element method for nonlinear fourth-order wave equations, *Appl. Numer. Math.*, **183** (2023), 333–354. https://doi.org/10.1016/j.apnum.2022.09.011

19. Y. Shi, X. Yang, Pointwise error estimate of conservative difference scheme for supergeneralized viscous Burgers equation, *Electron. Res. Arch.*, **32** (2024), 1471–1497. https://doi.org/10.3934/era.2024068

20. D. Furihata, Finite-difference schemes for nonlinear wave equation that inherit energy conservation property, *J. Comput. Appl. Math.*, **134** (2001), 37–57. https://doi.org/10.1016/S0377-0427(00)00527-6

21. Y. Liao, L. B. Liu, L. Ye, T. Liu, Uniform convergence analysis of the BDF2 scheme on Bakhvalov-type meshes for a singularly perturbed Volterra integro-differential equation, *Appl. Math. Lett.*, **145** (2023), 108755. https://doi.org/10.1016/j.aml.2023.108755

22. Z. Zhou, H. Zhang, X. Yang, CN ADI fast algorithm on non-uniform meshes for the three-dimensional nonlocal evolution equation with multi-memory kernels in viscoelastic dynamics, *Appl. Math. Comput.*, **474** (2024), 128680. https://doi.org/10.1016/j.amc.2024.128680

23. Y. O. Tijani A. R. Appadu, Unconditionally positive NSFD and classical finite difference schemes for biofilm formation on medical implant using Allen-Cahn equation, *Demonstratio Math.*, **55** (2022), 40–60. https://doi.org/10.1515/dema-2022-0006

24. H. Zhang, X. Yang, Y. Liu, Y Liu, An extrapolated CN-WSGD OSC method for a nonlinear time fractional reaction-diffusion equation, *Appl. Numer. Math.*, **157** (2020), 619–633. https://doi.org/10.1016/j.apnum.2020.07.017

25. X. Yang, Z. Zhang, Analysis of a new NFV scheme preserving DMP for two-dimensional sub-diffusion equation on distorted meshes, *J. Sci. Comput.*, **99** (2024), 80. https://doi.org/10.1007/s10915-024-02511-7

26. S. F. Bradford, B. F. Sanders, Finite-volume models for unidirectional, nonlinear, dispersive waves, *J. Waterw. Port. Coast.*, **128** (2002), 173–182. https://doi.org/10.1061/(ASCE)0733-950X(2002)128:4(173)

27. X. Yang, Z. Zhang, On conservative, positivity preserving, nonlinear FV scheme on distorted meshes for the multi-term nonlocal Nagumo-type equations, *Appl. Math. Lett.*, **150** (2024), 108972. https://doi.org/10.1016/j.aml.2023.108972

28. J. Shen, T. Tang, L. Wang, *Spectral Methods: Algorithms, Analysis and Applications*, Springer Science Business Media, 2011.

29. M. Dehghan, A. Taleei, Numerical solution of nonlinear Schrödinger equation by using time-space-pseudo-spectral method, *Numer. Meth. Part. Differ. Equations: Int. J.*, **26** (2010), 979–992. https://doi.org/10.1002/num.20468

30. T. Lu, W. Cai, A Fourier spectral-discontinuous Galerkin method for time-dependent 3-D Schrödinger-Poisson equations with discontinuous potentials, *J. Comput. Appl. Math.*, **220** (2008), 588–614. https://doi.org/10.1016/j.cam.2007.09.025

31. Y. Shi, X. Yang, A time two-grid difference method for nonlinear generalized viscous Burgers equation, *J. Math. Chem.*, **62** (2024), 1323–1356. https://doi.org/10.1007/s10910-024-01592-x

32. M. Yao, Z. Weng, A numerical method based on operator splitting collocation scheme for nonlinear Schrödinger equation, *Math. Comput. Appl.*, **29** (2024), 6. https://doi.org/10.3390/mca29010006

33. K. J. Ansari, M. Izadi, S. Noeiaghdam, Enhancing the accuracy and efficiency of two uniformly convergent numerical solvers for singularly perturbed parabolic convection- diffusion-reaction problems with two small parameters, *Demonstratio Math.*, **57** (2024), 20230144. https://doi.org/10.1515/dema-2023-0144

34. Z. Guan, C. Wang, S. M. Wise, A convergent convex splitting scheme for the periodic nonlocal Cahn-Hilliard equation, *Numer. Math.*, **128** (2014), 377–406. https://doi.org/10.1007/s00211-014-0608-2

35. Z. Guan, J. S. Lowengrub, C. Wang, S. M. Wise, Second order convex splitting schemes for periodic nonlocal Cahn-Hilliard and Allen-Cahn equations, *J. Comput. Phys.*, **277** (2014), 48–71. https://doi.org/10.1016/j.jcp.2014.08.001

36. J. Shen, C. Wang, X. Wang, S. M. Wise, Second-order convex splitting schemes for gradient flows with Ehrlich-Schwoebel type energy: application to thin film epitaxy, *SIAM J. Numer. Anal.*, **50** (2012), 105–125. https://doi.org/10.1137/110822839

37. X. Feng, T. Tang, J. Yang, Stabilized Crank-Nicolson/Adams-Bashforth schemes for phase field models, *East Asian J. Appl. Math.*, **3** (2013), 59–80. https://doi.org/10.4208/eajam.200113.220213a

38. J. Shen, X. Yang, Numerical approximations of Allen-Cahn and Cahn-Hilliard equations, *Discrete Contin. Dyn. Syst.*, **28** (2010), 1669–1691. https://doi.org/10.3934/dcds.2010.28.1669

39. L. Ju, X. Li, Z. Qiao, H. Zhang, Energy stability and error estimates of exponential time differencing schemes for the epitaxial growth model without slope selection, *Math. Comput.*, **87** (2018), 1859-1885. https://doi.org/10.1090/mcom/3262

40. L. Ju, J. Zhang, Q. Du, Fast and accurate algorithms for simulating coarsening dynamics of Cahn-Hilliard equations, *Comput. Mater. Sci.*, **108** (2015), 272–282. https://doi.org/10.1016/j.commatsci.2015.04.046

41. J. Zhao, Q. Wang, X. Yang, Numerical approximations for a phase field dendritic crystal growth model based on the invariant energy quadratization approach, *Int. J. Numer. Meth. Eng.*, **110** (2017), 279–300. https://doi.org/10.1002/nme.5372

42. J. Shen, J. Xu, Convergence and error analysis for the scalar auxiliary variable (SAV) schemes to gradient flows, *SIAM J. Numer. Anal.*, **56** (2018), 2895–2912. https://doi.org/10.1137/17M1159968

43. J. Shen, J. Xu, J. Yang, A new class of efficient and robust energy stable schemes for gradient flows, *SIAM Rev.*, **61** (2019), 474–506. https://doi.org/10.1137/17M1150153

44. Z. Liu, X. Li, The exponential scalar auxiliary variable (E-SAV) approach for phase field models and its explicit computing, *SIAM J. Sci. Comput.*, **42** (2020), B630–B655. https://doi.org/10.1137/19M1305914

45. F. Huang, J. Shen, Z. Yang, A highly efficient and accurate new scalar auxiliary variable approach for gradient flows, *SIAM J. Sci. Comput.*, **42** (2020), A2514–A2536. https://doi.org/10.1137/19M1298627

46. Z. Liu, X. Li, A highly efficient and accurate exponential semi-implicit scalar auxiliary variable (ESI-SAV) approach for dissipative system, *J. Comput. Phys.*, **447** (2021), 110703. https://doi.org/10.1016/j.jcp.2021.110703
47. C. Jiang, W. Cai, Y. Wang, A linearly implicit and local energy-preserving scheme for the sine-Gordon equation based on the invariant energy quadratization approach, *J. Sci. Comput.*, **80** (2019), 1629–1655. https://doi.org/10.1007/s10915-019-01001-5
48. D. Li, W. Sun, Linearly implicit and high-order energy-conserving schemes for nonlinear wave equations, *J. Sci. Comput.*, **83** (2020), 1–17. https://doi.org/10.1007/s10915-020-01245-6
49. N. Wang, M. Li, C. Huang, Unconditional energy dissipation and error estimates of the SAV Fourier Spectral Method for nonlinear fractional generalized wave equation, *J. Sci. Comput.*, **88** (2021), 19. https://doi.org/10.1007/s10915-021-01534-8
50. F. Yu, M. Chen, Error analysis of the Crank-Nicolson SAV method for the Allen-Cahn equation on variable grids, *Appl. Math. Lett.*, **125** (2022), 107768. https://doi.org/10.1016/j.aml.2021.107768
51. L. Ju, X. Li, Z. Qiao, Stabilized exponential-SAV schemes preserving energy dissipation law and maximum bound principle for the Allen-Cahn type equations, *J. Sci. Comput.*, **92** (2022), 66. https://doi.org/10.1007/s10915-022-01921-9